

# Development of Natural Hydrophobic Deep Eutectic Solvents for Precombustion CO<sub>2</sub> Capture

Kun Xin, Fausto Gallucci, and Martin van Sint Annaland\*



Cite This: *ACS Sustainable Chem. Eng.* 2022, 10, 15284–15296



Read Online

ACCESS |

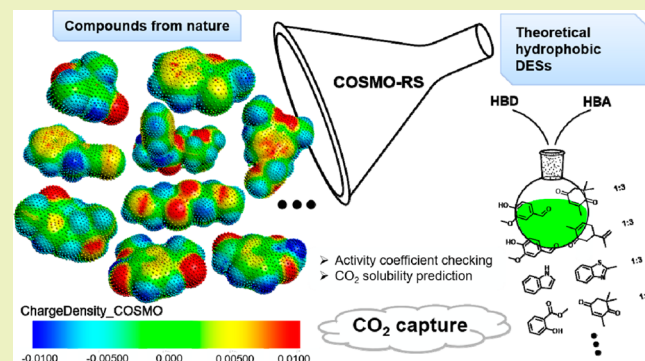
Metrics & More

Article Recommendations

Supporting Information

**ABSTRACT:** Hydrophobic deep eutectic solvents (DESS) have been designed as effective solvents for precombustion CO<sub>2</sub> capture by using a conductor-like screening model for real solvents (COSMO-RS). Reliable CO<sub>2</sub> solubilities in various compounds and binary solvents were estimated. We have developed new DESS from 38 selected, nature-derived, hydrophobic, and CO<sub>2</sub> affinitive compounds. The possibilities of any two of these substances to form DESS were assessed from predicted activity coefficients, followed by an estimation of the CO<sub>2</sub> solubilities of the theoretically feasible DESS. 58 promising hypothetical DESS were screened out. Subsequently, eight DESS were successfully prepared and characterized. Most of these DESS have a density larger than 1.0 g/mL at 298.15 K. The DESS have a similarly low volatility as decanoic acid–menthol (1:2) and are thermally stable below 420 K. Vanillin-4-oxoisophorone (1:3) and methyl salicylate-4-oxoisophorone (1:1) have been identified to be very promising for precombustion capture, showing comparable CO<sub>2</sub> solubility and viscosity to the well-known, conventionally used Selexol solvent.

**KEYWORDS:** Precombustion, Hydrophobic deep eutectic solvents, COSMO-RS, CO<sub>2</sub> solubility, Density, 4-Oxoisophorone



## INTRODUCTION

CO<sub>2</sub> capture from energy intensive industries, including power plants, is regarded as an effective midterm solution to reduce anthropogenic greenhouse gas emissions. In this respect, the development of advanced low carbon-intensive power plants, based on the integrated gasification combined cycle (IGCC) with carbon capture is a promising technology to decarbonize the power production sector.<sup>1</sup> At a gasification plant, fossil fuels are converted to a syngas containing mainly H<sub>2</sub>, CO, CO<sub>2</sub>, and H<sub>2</sub>O. Generally, the syngas is then processed in water–gas shift (WGS) reactors, and the product is sent for desulphurization and CO<sub>2</sub> separation. Physical absorbents are commonly used driven by the high partial pressure of CO<sub>2</sub>,<sup>2</sup> because they can be regenerated with a relatively low energy demand through depressurization.

Among various candidates of physical absorption technologies, the Selexol process has been commercialized and widely applied. Selexol consists of a mixture of dimethyl ether polyethylene glycols (DEPG), with the chemical formula CH<sub>3</sub>O(C<sub>2</sub>H<sub>4</sub>O)<sub>n</sub>CH<sub>3</sub>, where *n* ranges from 2 to 9. According to a National Energy Technology Laboratory (NETL) report,<sup>3</sup> a dual-stage Selexol process combined with an IGCC power plant (90% capture rate) will increase the power generation cost by about 30%. Additionally, the emission of evaporated absorbent into the atmosphere results in harmful effects on the environment and human health. For these reasons, several

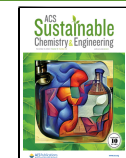
novel, more environmentally friendly solvents have been developed to improve the absorption performance. Ionic liquids (ILs) are considered promising solvents because of their advantageous properties such as negligible vapor pressure, low melting point, high thermal stability, and adjustable properties. However, traditional ILs suffer from the disadvantages of high production costs and toxicity. At the beginning of this century, a new generation of solvents, named deep eutectic solvents (DESS), have attracted a great amount of attention as an alternative to ILs, owing to their relatively low cost, while being nontoxic, biodegradable, and designable.<sup>4</sup> The so-called natural deep eutectic solvents (NADESs) made from natural or bioderived constituents have aroused particular interest from researchers.<sup>5</sup>

Recently, a number of nonionic DESS<sup>5</sup> were developed as water-immiscible extractants. Their hydrophobicity and tunable physicochemical properties made them promising for CO<sub>2</sub> physical absorption.<sup>6</sup> In fact, before gas enters the Selexol unit, the dehydration of the feed gas is required,<sup>7</sup> because

Received: August 25, 2022

Revised: October 28, 2022

Published: November 9, 2022



water accumulation in the absorbent can cause a detrimental effect on the absorption capacity and metal corrosion. The use of hydrophobic solvents not only prevents water accumulation but also allows operation at higher absorption temperatures.<sup>8</sup> According to process modeling results by NETL,<sup>9</sup> a typical IGCC fuel gas stream (31 mol % CO<sub>2</sub>, 43% H<sub>2</sub>, 23% H<sub>2</sub>O, and 3% of other gases such CO, COS, H<sub>2</sub>S) leaves the WGS reactor at 250 °C and 5.5 MPa. If CO<sub>2</sub> can be selectively removed from the stream using hydrophobic solvents with little or no cooling and water remains in the gas phase, then the combustion of the H<sub>2</sub>–H<sub>2</sub>O gas mixture in the gas turbine system will result in an increase of 2–3 percentage points in the IGCC plant thermal efficiency.

Recently, several DESs with high CO<sub>2</sub> capacity have been reported,<sup>10–12</sup> but none of them can outperform the Selexol solvent from an economic perspective. Due to the enormous number of possible combinations between a hydrogen bond donor (HBD) and a hydrogen bond acceptor (HBA), a vast number of possible DESs need to be synthesized and characterized, because until now the development of new DESs has followed a trial and error process.

Considering that the CO<sub>2</sub> solubility is the most important property for precombustion capture,<sup>6</sup> researchers can focus more on developing DESs with a high CO<sub>2</sub> solubility, but it is still an incredible amount of work to prepare and identify the most appropriate DESs for CO<sub>2</sub> capture based on experimental measurements only. This highlights the clear potential of a rapid and a priori screening tool to predict the CO<sub>2</sub> solubility of DESs. It should be noted that many functionalized DESs can chemically capture CO<sub>2</sub> and hold great promise for postcombustion capture. Interested readers can refer to anion-functionalized DESs like azolide-based DESs,<sup>13</sup> superbase-based DESs like the mixture of biophenol-derived superbase ILs and ethylene glycol,<sup>14</sup> and hydrophobic polyamine-based DESs.<sup>15</sup> The group contribution method (GCM) and the conductor-like screening model for real solvents (COSMO-RS) are recommended for the prediction of several of the important thermodynamic properties of solvents.<sup>16</sup> In the GCM, the property of a compound is a function of structurally dependent parameters, which are determined by summing the number of each group present in the molecule times its contribution. Haghbakhsh et al.<sup>17</sup> proposed a simple correlation to predict the DES density. The model is a function of the critical temperature, critical volume, acentric factor, and system temperature, where the critical parameters are estimated by GCM.<sup>18</sup> Despite the efficiency and simple applicability, GCM has the disadvantage of doubtful accuracy when the molecular parameters are lacking or questionable, caused by the absence or very limited availability of experimental data required for the fitting of the required group interaction parameters. On the other hand, the COSMO-RS model is based on quantum mechanics and requires only information on the molecular structure as input. Lemaoui et al.<sup>19</sup> presented quantitative structure–property relationship (QSPR) models for the prediction of the density and viscosity of DESs using COSMO-RS based descriptors. CO<sub>2</sub> solubilities in different ammonium- and phosphonium-based ionic DESs were predicted with COSMO-RS and compared with experimental results for verification, as reported by Liu et al.<sup>20</sup> and Alioui et al.<sup>21</sup> Similarly, Liu et al.<sup>22</sup> developed corrected COSMO-RS models to quantitatively predict CO<sub>2</sub> solubility in ammonium-based DESs.

The objective of the current work is to develop nonionic hydrophobic DESs with high CO<sub>2</sub> solubility for precombustion CO<sub>2</sub> capture, competitive with the conventional Selexol solvent. Based on the predictions for the CO<sub>2</sub> solubility in 70 different DESs, DESs proposed in the literature are screened. The COSMO-RS method is adopted as a screening tool, and its ability to provide an accurate prediction of the CO<sub>2</sub> solubility is validated beforehand. Subsequently, large efforts are paid to prepare new natural DESs. 38 naturally hydrophobic compounds with a high CO<sub>2</sub> affinity are selected, and the possibilities for any two components to form a DES are evaluated using their predicted individual activity coefficients. The CO<sub>2</sub> solubility in the theoretically feasible DESs is predicted, and the promising DESs are screened out. Lastly, eight DESs are prepared and characterized. Nuclear magnetic resonance (NMR) spectroscopy is used to verify whether reactions may occur during the preparation of the DESs. The CO<sub>2</sub> solubility in these DESs are measured with a magnetic suspension balance (MSB). The density, viscosity, volatility, thermal stability, and miscibility with water are also experimentally determined.

## THEORETICAL BACKGROUND

The COSMO-RS model is a quantum chemistry based equilibrium thermodynamics method, which defines chemical compounds and their mixtures in terms of a collection of surface segments. It views all molecular interactions as local pairwise interactions of surface segments.<sup>23</sup> A single quantum mechanical calculation is carried out to obtain the charge density of each surface panel of one molecule in an ideal conductor. With the distribution of the surface area as a function of the charge density, the so-called sigma profile, the COSMO-RS model is able to calculate the chemical potential of an arbitrary solute in any pure or mixed solvent, enabling the prediction of various properties. With the chemical potential of a compound in a mixture being calculated, the activity coefficient in the liquid solution  $\gamma_i$  is presented in eq 1,

$$\gamma_i = \exp\{(\mu_i^{\text{solv}} - \mu_i^{\text{pure}})/RT\} \quad (1)$$

where  $\mu_i^{\text{solv}}$  and  $\mu_i^{\text{pure}}$  are the chemical potential of compound  $i$  in the reference state of the mixture and the pure compound, respectively. Subsequently, the gas solubility (mole fraction) for systems at subcritical conditions and low pressures can be determined.<sup>24,25</sup> Then Henry's constant can be determined by dividing the fugacity of CO<sub>2</sub> by its mole fraction in the liquid. The gas phase above the DES has been assumed to be pure CO<sub>2</sub>, and its fugacity was calculated with the Peng–Robinson equation of state in Aspen Plus (version 11.0). By combining the CO<sub>2</sub> mole fraction, molecular weights of CO<sub>2</sub> and solvent, as well as the liquid density, the CO<sub>2</sub> solubility (in g/L) was calculated. Volume expansion during the absorption was not taken into account. The liquid density of the DES containing dissolved CO<sub>2</sub> is assumed to be the same as the DES density without CO<sub>2</sub> dissolved (eq 7). The pure compound density is computed from a quantum structure–property relationship (QSPR), by mapping various QSPR descriptors of an input molecule onto a single numerical value. For more details on the COSMO-RS method, the interested reader is referred to the work by Palomar et al.<sup>26</sup>

The quantum COSMO-RS calculations were performed with the Amsterdam Density Functional (ADF) version 2019.301. For the compounds that exist in the COSMO-RS

Database ADFCRS-2018, the COSMO result files were used without any modification. For other substances, the molecule was created in ADF, and geometry optimizations of the molecule were performed using the generalized gradient approximation—the Becke Perdew exchange correlation functional (GGA:BP86) and the zero order regular approximation (ZORA) were adopted to treat the relativistic effects. The TZP small core basis set and an integration accuracy with a good quality were used. The COSMO files containing the ideal screening charges on the molecular surface were generated. For more details on the procedures to prepare the data and to predict thermodynamic properties, readers are referred to the SCM Web site.<sup>24,27</sup>

To evaluate the accuracy of the model predictions, the discrepancies between the estimated property value with COSMO-RS and the corresponding experimental data points were quantified with the average absolute relative deviation (AARD), presented in eq 2, where NP is the total number of data points,  $x_{i,\text{exp.}}$  is the experimental CO<sub>2</sub> mole fraction in a solvent at given temperature and pressure, and  $x_{i,\text{pred.}}$  is the corresponding predicted result.

$$\text{AARD\%} = \frac{100}{\text{NP}} \sum_{i=1}^{\text{NP}} \left| \frac{x_{i,\text{exp.}} - x_{i,\text{pred.}}}{x_{i,\text{exp.}}} \right| \quad (2)$$

## EXPERIMENTAL SECTION

**Materials and DESs.** The chemicals used in the experimental part of this work, including their source, purity, and molecular structures, have been summarized in Table 1. All chemicals were used as received from the supplier.

**DESs Preparation.** The desired molar ratio of two selected compounds, one HBD and one HBA, were weighed and mixed in a vial. The vial was stirred and heated to 50 °C by IKA RCT basic magnetic stirrers. The DES was obtained and remained a clear liquid at room temperature.

**NMR Analysis.** <sup>1</sup>H NMR spectra were recorded at ambient temperature using a Bruker Advance 400 MHz spectrometer with 16 scans. <sup>1</sup>H NMR spectra are reported in parts per million (ppm) downfield relative to CDCl<sub>3</sub> (7.26 ppm).

**CO<sub>2</sub> Solubility Measurement.** The solubility of CO<sub>2</sub> in DESs was studied by determining the bubble-point curve using a magnetic suspension balance (MSB, Rubotherm GmbH). The MSB and the experimental procedures have been described by Zubeir et al.<sup>28</sup> The same setup was used in this work. During the measurements, the mass of the sample was weighed with a high-resolution microbalance (0.01 mg). The CO<sub>2</sub> solubility isotherms were measured at 298.15 and 313.15 K in the pressure range from 0.1 to 2 MPa. The mass of the dissolved CO<sub>2</sub>, taking the buoyancy effect into account, was obtained by

$$m_{\text{CO}_2} = m_{\text{bal}}(P) - m_{\text{sc+s}} + V_{\text{sc+s+CO}_2} \cdot \rho_{\text{CO}_2}(P) \quad (3)$$

where  $m_{\text{CO}_2}$  is the mass of CO<sub>2</sub> dissolved,  $m_{\text{bal}}$  is the reading of the balance,  $m_{\text{sc+s}}$  is the total mass of the loaded sample container,  $V_{\text{sc+s+CO}_2}$  is the sum of the CO<sub>2</sub> rich solvent and sample container volume, and  $\rho_{\text{CO}_2}(P)$  is the density of CO<sub>2</sub> at the measurement conditions. Assuming that the volume of the CO<sub>2</sub> absorbed is insignificant, eq 3 is reduced to

$$m_{\text{CO}_2} = m_{\text{bal}}(P) - m_{\text{sc+s}} + V_{\text{sc+s}} \cdot \rho_{\text{CO}_2}(P) \quad (4)$$

The CO<sub>2</sub> mole fraction absorbed  $x_{\text{CO}_2}$  is determined from

**Table 1. Chemicals Used in the Experimental Part, Including Their Molecular Structure, Source, CAS Number, and Purity**

Component	Molecular structure	Source	CAS number	Purity (%)
4-oxoisophorone		TCI chemicals	1125-21-9	>98
vanillin		TCI chemicals	121-33-5	>98
methyl salicylate		TCI chemicals	119-36-8	>99
benzyl isothiocyanate		TCI chemicals	622-78-6	>98
carvone		TCI chemicals	6485-40-1	>99
2-methylbenzothiazole		Sigma-Aldrich	120-75-2	>99
indole		TCI chemicals	120-72-9	>99
2,3,5,6-tetramethylpyrazine		TCI chemicals	1124-11-4	>98
menthol		TCI chemicals	89-78-1	>98

$$x_{\text{CO}_2} = \frac{\frac{m_{\text{CO}_2}}{\text{MW}_{\text{CO}_2}}}{\frac{m_{\text{CO}_2}}{\text{MW}_{\text{CO}_2}} + \frac{m_s}{\text{MW}_s}} \quad (5)$$

where MW<sub>CO<sub>2</sub></sub> is the molecular weight of CO<sub>2</sub> (44.01 g·mol<sup>-1</sup>), and MW<sub>s</sub> is the molecular weight of the DES sample. Good repeatability was found for the measured CO<sub>2</sub> mole fractions in the liquid (see Figure S1).

**Density and Viscosity Measurements.** The viscosity and density of screened DESs were measured between 293.15 and 353.15 K by a Lovis 2000 M/ME micro-viscometer (Anton Paar, Austria). It is a rolling-ball viscometer which measures the rolling time of a ball through liquids. A glass capillary with an inner diameter of 1.8 mm equipped with a gold-coated ball was used. The capillary was calibrated with a N26 synthetic base oil, which was supplied by Paragon Scientific Limited. The variation coefficient of the dynamic viscosity was below 0.2%.

**Water Solubility Measurement.** 3.0 g of deionized water was weighed in a 10 mL vial, and then 3.0 g of hydrophobic DES was added. A stir bar mixed the solution with a magnetic stirrer for 1 h, and then the mixture was left to settle overnight. The DES phase was taken with a needled syringe to analyze its water content afterward. The water content was determined with a D39 Coulometric Karl Fischer titration apparatus from Mettler Toledo. For each DES, the average value of three consecutive measurements at room temperature (22 ± 1 °C) was taken. A GCMS-QP2010 (Shimadzu Corporation) connected to a Shimadzu AOC-20s Autosampler was used to determine the DES content in the water phase. About 0.85 g of the water phase was taken with another syringe and mixed with 0.05 g of

ethanol. A 1  $\mu\text{L}$  liquid sample was injected automatically at the injection temperature of 523.15 K. The ion-source temperature was 473.15 K. GC-2010 Plus was equipped with a capillary column (SH-Rxi-1ms, 30 m  $\times$  0.25 mm  $\times$  0.25  $\mu\text{m}$ , coated with 100% dimethylpolysiloxane). The column temperature was programmed as follows: after 5.0 min of maintaining the temperature at 353.15 K, the column temperature was raised to 523.15 K at a rate of 20 K/min and was kept at this temperature for 4.0 min. The internal standard method was used to obtain quantitative results in the analysis, and ethanol was chosen as the internal standard. The relative response factor of the DES constituent with respect to ethanol was determined with an equal-mass DES + ethanol mixture.

**Volatility Determination.** As shown in previous work,<sup>29</sup> a plot of the vapor pressure ( $p^{\text{vap}}$ ) and a parameter ( $\nu$ ) follows the same linear trend (eq 6) for a series of compounds with known vapor pressure, regardless of their chemical structure.

$$p^{\text{vap}} = k \cdot \nu \quad (6)$$

where  $\nu$  can be determined with thermogravimetric analysis (TGA). Methyl salicylate was used as the reference substance. The total vapor pressure of four DESs at 298.15 and 313.15 K was determined in this work.

**Thermal Stability.** The stability of the DESs at elevated temperatures was investigated with a laboratory-assembled TGA, with a temperature and weight accuracy of  $\pm 1$  K and 0.05 mg, respectively. Experiments were carried out under a constant nitrogen flow rate of 30 mL/min. A sample of 60–90 mg was held in a stainless steel basket and was heated at a rate of 10 K·min<sup>-1</sup> from 298.15 to 673.15 K. The temperature-programmed thermogravimetric analyses were used to determine the degradation temperature<sup>30</sup> of eight promising novel hydrophobic DESs.

## RESULTS AND DISCUSSION

**Accuracy of CO<sub>2</sub> Solubility Prediction with COSMO-RS.** COSMO-RS is based on the assumptions of an incompressible liquid and an ideal gas phase.<sup>31</sup> All predictions in this work were made for systems over the temperature range 273.15–323.15 K and a pressure range 0–20 bar, where the gas can be considered as an ideal gas. The gas pressure over the solvent was converted to fugacity using the Peng–Robinson equation in Aspen Plus (version 11.0). The calculation of gas solubility with COSMO-RS in a solvent requires the vapor pressure of the pure compound. Two calculation strategies were adopted. In Method 1, the vapor pressure determined from gas-phase energy information from the DFT calculations<sup>32</sup> in ADF was used for the prediction of the gas solubility via COSMO-RS. For Method 2, the pure compound vapor pressure was estimated with the QSPR model.

Henry's constant for CO<sub>2</sub> in a variety of pure solvents was predicted. The parity plots of model predictions and experimental data in chain alkanes and alkenes, naphthenes and aromatics, alcohols, ketones, esters, ethers and acids, amides, other N-containing compounds, as well as P and S containing compounds are presented in Figure 1a–i, respectively. The details of the solvents are summarized in Table S1 in the Supporting Information, and the experimental data in Figure 1 was collected from the literature.<sup>33–45</sup> Henry's constants for CO<sub>2</sub> in pure solvents predicted with Method 1 and 2 are represented by the black and red markers, respectively. From the parity plots, it can be concluded that Henry's constants for CO<sub>2</sub> predicted from the DFT calculations are consistently somewhat higher compared to Henry's constants predicted when estimating the vapor pressure with the QSPR model. Moreover, as shown in Figure 1b,g, most of the points are below the line  $y = x$ , demonstrating that Henry's constants for cyclic compounds and amides are

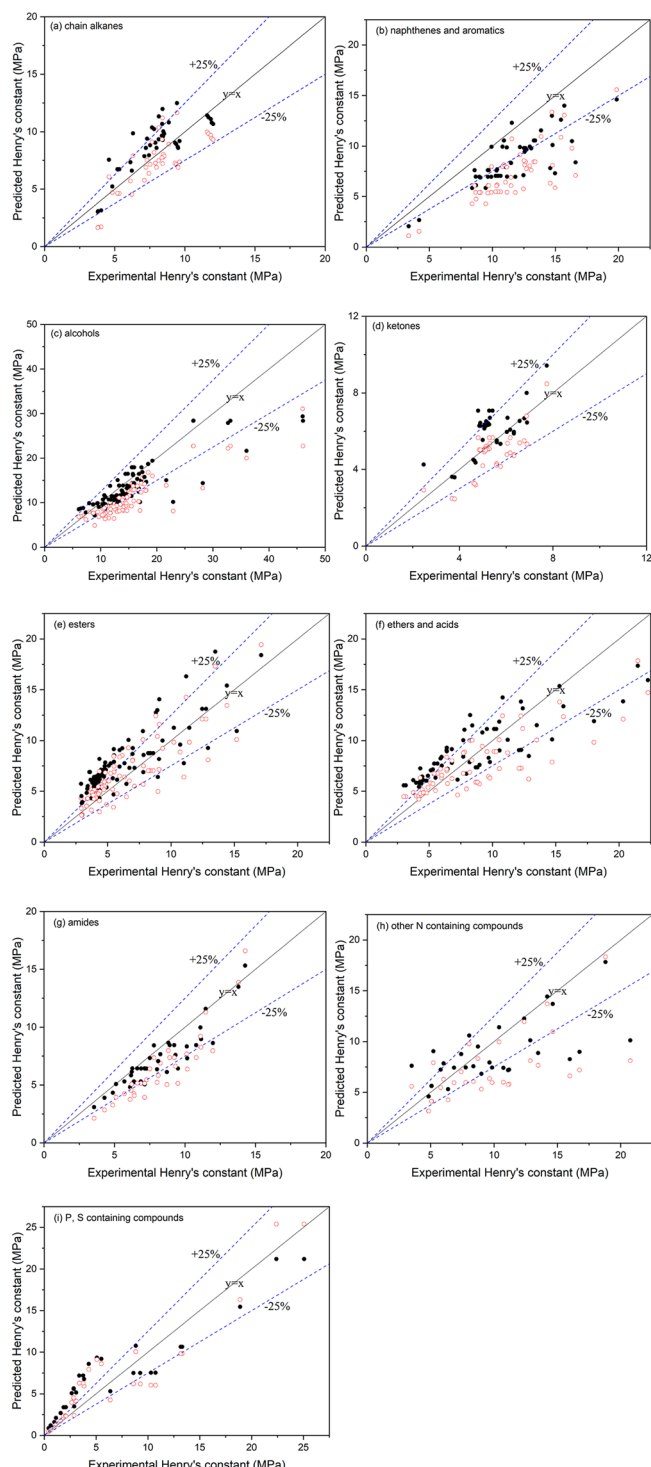


**Figure 1.** Parity plots of model predictions and experimentally determined Henry's constants of CO<sub>2</sub> in (a) chain alkanes and alkenes, (b) naphthenes and aromatics, (c) alcohols, (d) ketones, (e) esters, (f) ethers and acids, (g) amides, (h) other N containing compounds, as well as (i) P, S containing compounds. Prediction results by Method 1 and 2 are represented with black and red markers, respectively. Relative deviations of 25% are shown with straight lines passing through the origin.

underpredicted by COSMO-RS. This could be caused by inaccurate parametrization in COSMO-RS, particularly specific parameters for element N. Nevertheless, overall, for both methods, and especially for Method 1, acceptable predictions

are obtained for the majority of the investigated components, where mostly the discrepancy with experimental data is within about 25%.

$\text{CO}_2$  solubilities in several dual solvent systems were also estimated and compared with literature values. The investigated systems include methanol + water,<sup>46</sup> ethanol + water,<sup>47</sup> acetone + water,<sup>48</sup> dimethylformamide + water,<sup>49</sup> cyclohexane + cyclohexanone,<sup>50</sup> phenol + water,<sup>51</sup> dimethyl sulfoxide + ethylene glycol,<sup>52</sup> acetic acid + vinyl acetate, dimethyl carbonate + propylene carbonate,<sup>53</sup> acetone + methanol,<sup>54</sup> dimethyl carbonate + ethylene carbonate, dimethyl carbonate + diethyl carbonate, and dimethyl carbonate + propyl acetate.<sup>55</sup> A wide range of compositions were considered for each system. For example, for the methanol + water system, the mass fraction of methanol was varied from 5 to 100%. The parity plots of the model predictions and experimental data for the  $\text{CO}_2$  solubility in the above-mentioned mixtures are shown in Figures 2 and S2, where Method 1 and 2 have been used for

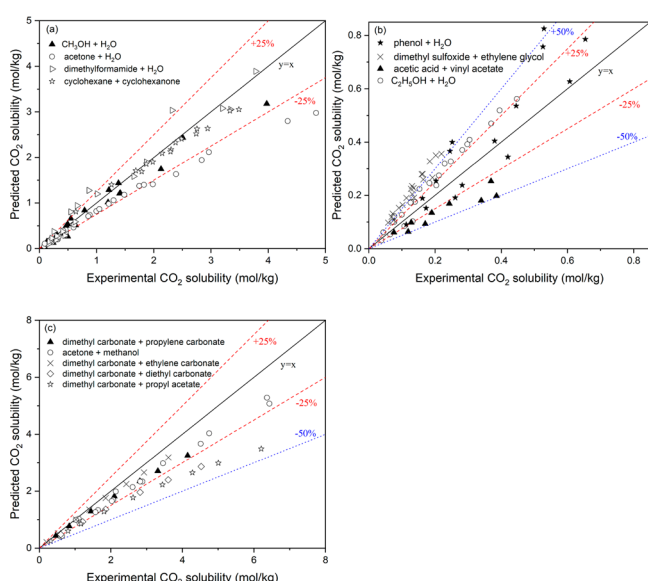


**Figure 2.** Panels a–c show the parity plots of model predictions (with Method 1) and experimentally determined  $\text{CO}_2$  solubilities for various binary mixtures. Specific relative deviations are shown with straight lines passing through the origin.

the COSMO-RS calculations, respectively. Large deviations were found for the mixture of dimethyl sulfoxide + ethylene glycol, where the absolute relative error is larger than 50%, as shown in Figure 2b. But it should be pointed out that

experimental errors could also account for part of the deviations. The Henry's constant for  $\text{CO}_2$  in ethylene glycol<sup>34</sup> is 47.68 MPa at 298.15 K, while the value of 26.55 MPa is recommended in the literature.<sup>33</sup> Consistent with the prediction results for pure solvents, higher  $\text{CO}_2$  solubilities are predicted by Method 2 than by Method 1. Experimental measurements of the  $\text{CO}_2$  solubility in various DESs are costly and time-consuming. Overall, the deviations between COSMO-RS predictions and the relevant experimental data for pure solvents and binary mixtures are deemed acceptable for screening-level evaluations.

**Screening of Nonionic DESs from the Literature.** 70 nonionic DESs were selected from a recent review.<sup>56</sup> Mass fractions of  $\text{CO}_2$  in these DESs at 273.15, 298.15, and 313.15 K under 0.1 and 2.0 MPa were predicted with Method 1. The detailed prediction results are summarized in Table S2. Temperature and pressure have little impact on the ranking of the DESs. The highest  $\text{CO}_2$  mass fraction is found in acetic acid–menthol (2:1) for all the investigated conditions. Propionic acid–menthol (2:1) is the DES with the second-largest  $\text{CO}_2$  mass fraction under most conditions except at 273.15 K and 2.0 MPa, where a slightly larger  $\text{CO}_2$  mass fraction of 0.1514 is found in menthol–camphor (1:1). The same was observed for acrylic acid–menthol (2:1) and menthol–camphor (1:1), where the latter has a higher  $\text{CO}_2$  solubility under most conditions.

Not only is the  $\text{CO}_2$  mass fraction in DESs an important factor, but also the liquid density is a crucial solvent property. A solvent with a high  $\text{CO}_2$  mass solubility but with a low density may not be preferable. For equal mass solubility, a higher density of the DES means that a smaller liquid volume is required with a consequently smaller size of the absorber and regeneration facilities, reducing the capital cost. Therefore, the mass fraction of  $\text{CO}_2$  in each DES at 298.15 K was converted into the mass of  $\text{CO}_2$  that was dissolved per liter using the predicted density, where the densities of the DESs were estimated with COSMO-RS in ADF. The accuracy of the density prediction is discussed in the last section of this paper. The mass concentrations of  $\text{CO}_2$  are also presented in Table S2. Taking the two DESs decanoic acid–menthol (1:1) and thymol–lidocaine (1:1) as an example, the predicted densities are 0.881 and 0.961 g/mL at 298.15 K, versus experimental data of 0.900 and 0.993 g/mL,<sup>56</sup> respectively. A reasonably accurate prediction of the density is obtained for both DESs, with an absolute relative deviation of 2.11 and 3.22%, respectively. A larger density was estimated for thymol–lidocaine (1:1). Therefore, although a larger  $\text{CO}_2$  mass fraction of 0.068 was found for decanoic acid–menthol (1:1) at 298.15

**Table 2. Comparison of the Properties of the Selected DESs from the Literature<sup>56,57,60</sup> with Selexol at 298.15 K**

solvent	density (g/mL)		predicted $\text{CO}_2$ solubility under 2.0 MPa		
	experimental	predicted	mass fraction (%)	mass concentration (g/L)	experimental viscosity (cP)
acetic acid–menthol (2:1)	0.98	0.910	9.27	92.98	6.12
propionic acid–menthol (2:1)	NA <sup>b</sup>	0.909	8.99	89.79	NA
menthol–camphor (1:1)	0.924	0.899	8.88	87.68	16.42
acrylic acid–menthol (2:1)	NA	0.907	8.70	86.45	NA
acetic acid–menthol (1:1)	0.931	0.905	8.88	88.21	19.46
methanoic acid–menthol (1:1)	0.92	0.930	8.63	87.85	10.74
Selexol solvent	1.03	NA	10.79 <sup>a</sup>	111.15 <sup>a</sup>	5.8
deca-N8888Br (2:1) <sup>58</sup>	0.930	NA	5.83	51.49	469 (at 303.15 K)

<sup>a</sup>Interpolated value from experimental data at 8.0 and 14.5 bar. <sup>b</sup>Not available.

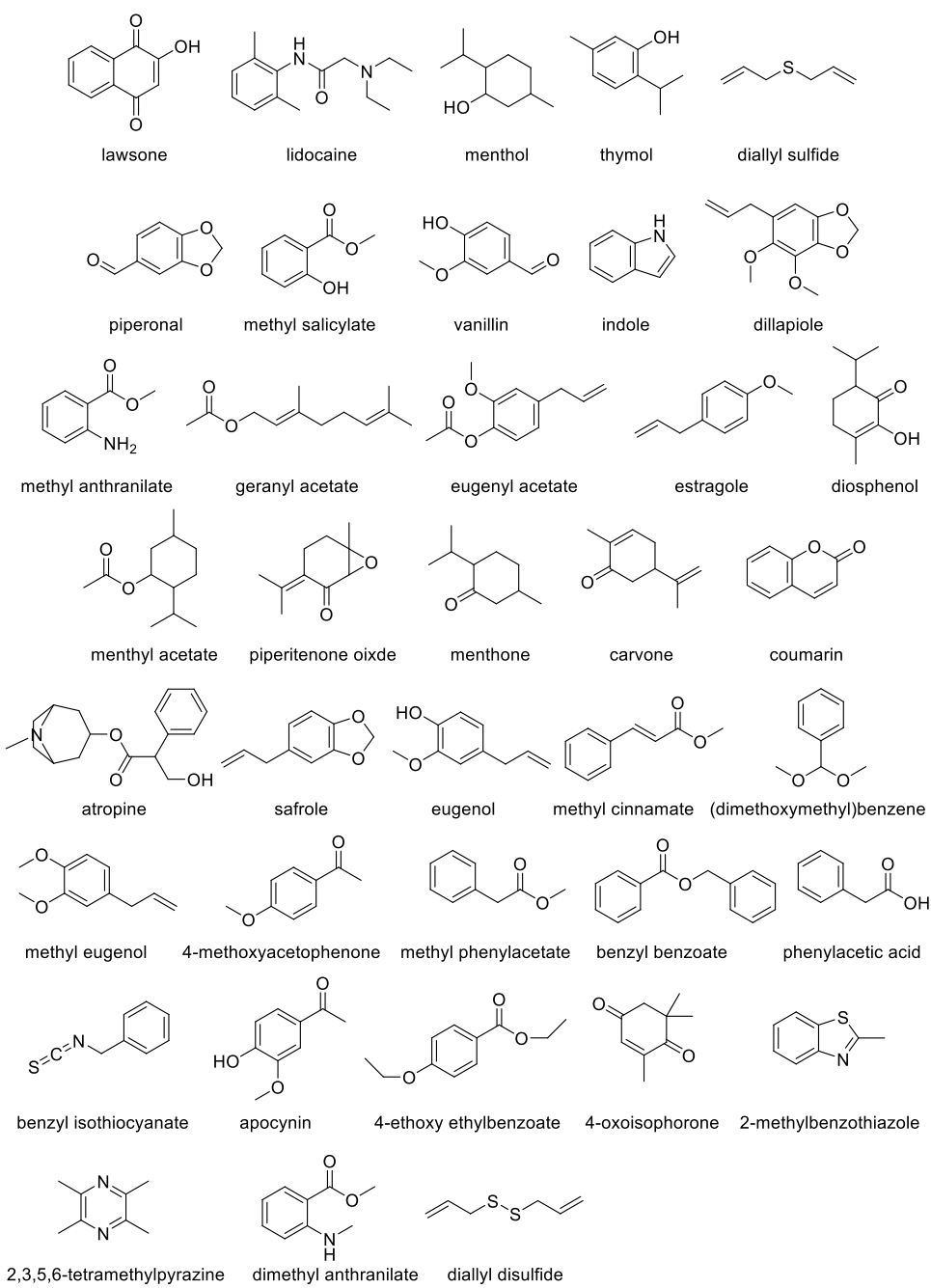


**Figure 3.** 38 natural compounds screened out from essential oils for new DES development.

K under 2.0 MPa, a smaller mass concentration of 64.11 (g CO<sub>2</sub>)/(L solvent) is calculated. The estimated CO<sub>2</sub> mass fraction and mass concentration in thymol–lidocaine (1:1) under the same conditions are 0.060 and 67.68 (g CO<sub>2</sub>)/(L solvent), respectively. The 70 DESs were ranked in view of their CO<sub>2</sub> solubility under each condition. The best six DESs are all menthol-based. Properties of these solvents are summarized in Table 2, where the properties of the reference Selexol solvent<sup>57</sup> have also been included. The DESs were rated according to the CO<sub>2</sub> solubilities in these solvents. The specific rankings of the solvents are shown in Table S3. The viscosities of the selected DESs are of the same order of magnitude as Selexol. But lighter densities are estimated for these DESs, resulting in a larger difference in CO<sub>2</sub> mass concentration. In view of the CO<sub>2</sub> capacity, though the best

nonionic DESs from the literature present much higher CO<sub>2</sub> solubility than ionic ones,<sup>58</sup> they still cannot compete with Selexol. Moreover, in the selected DESs volatile substances like formic acid, acetic acid, propionic acid, and acrylic acid are used as DES constituents, bringing about large solvent loss problems. However, these hydrophobic DESs still outperform most hydrophilic DESs in view of CO<sub>2</sub> solubility. Song et al.<sup>59</sup> applied COSMO-RS to screen 461 experimentally reported DESs for CO<sub>2</sub> capture, and the best was found to be ChCl–ethylenecyanohydrin (1:2), with a Henry's constant of 0.99 MPa kg/mol. At 2.0 MPa (fugacity of 1.787 MPa), the mass concentration of CO<sub>2</sub> in this DES is estimated to be 79.44 g/L, lower than that in any hydrophobic DES in Table 2. For comparison, also Method 2 was adopted for the COSMO-RS calculations, and the same best six DESs were screened out in

terms of CO<sub>2</sub> solubility. The specific rankings of these 70 DESs are summarized in Table S4.

**Development of New Natural Hydrophobic DESs for CO<sub>2</sub> Capture.** Essential oils are natural compounds extracted from plants and can be found in roots, stems, leaves, flowers, or fruits. The hydrophobicity and diversity of their components have attracted our attention. In the literature, terpenes, the most widely represented class of hydrocarbons in essential oils, have shown great promise for the formation of eutectics.<sup>5</sup> Combining the fact that the carbonyl (>C=O, >C=S) and sulfonyl (>S=O, >S=S) compounds have a higher CO<sub>2</sub> affinity, strong  $\pi\cdots\pi$  linkages exist between CO<sub>2</sub> and aromatic rings, and the interaction of CO<sub>2</sub> with unsaturated hydrocarbons is stronger than that of CO<sub>2</sub> with saturated hydrocarbons,<sup>61</sup> 38 natural and CO<sub>2</sub> affinitive compounds have been selected out, where most of them are components of essential oils.<sup>62</sup> The selected components together with their corresponding chemical names are shown in Figure 3. The majority of the selected compounds have boiling points above 200 °C. Hypothetical DESs are obtained by mixing any two of these substances in a molar ratio of 1:1, and  $38 \times 37$  combinations were evaluated by the predicted activity coefficients of the DES constituents at 298.15 K. The DESs with activity coefficients smaller than 0.95 for both constituents were filtered and summarized in Table S5. The predicted activity coefficients can also provide information on the melting point of the DES.<sup>63</sup> Activity coefficients of pure compounds lower than 1 indicate a decrease in the melting point of the mixture. During the screening process, the estimated  $\sigma$ -profiles by COSMO-RS were used to distinguish the HBD and HBA for each combination. The  $\sigma$ -profile plots for a molecule can be categorized into three regions:<sup>64</sup> (I) the HBD region for  $\sigma < -0.0084 \text{ e } \text{\AA}^{-2}$ , (II) the HBA region for  $\sigma > 0.0084 \text{ e } \text{\AA}^{-2}$ , and (III) the nonpolar region for the intermediate range of  $-0.0084 \leq \sigma \leq 0.0084 \text{ e } \text{\AA}^{-2}$ . Take methyl salicylate–indole (1:1) for example, shown in Figure 4.

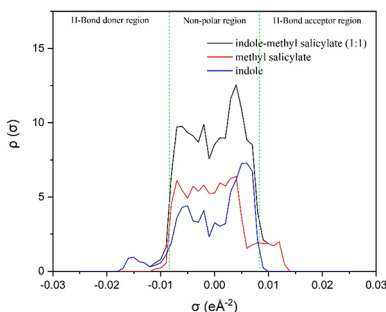


Figure 4.  $\sigma$ -Profile of indole–methyl salicylate (1:1) (black), methyl salicylate (red), and indole (blue).

HBD and HBA regions are found for indole and methyl salicylate, respectively. Apparently, indole and methyl salicylate are sufficiently polar to induce hydrogen bonding. 175 combinations were screened out in total.

Next, the CO<sub>2</sub> solubilities of the selected DESs at 298.15 K were estimated, where different molar ratios of 3:1 and 1:3 were considered for the HBD and HBA combinations. The predicted solubilities in 525 DESs are presented in Figure 5. Two red lines ( $y = 0.088$  and  $y = 100 \text{ g/L}$ ) are included in the plot to indicate the maximum performance of DESs reported in the literature (Table 2). 58 promising DESs with high CO<sub>2</sub> solubilities are screened from these simulations and are listed

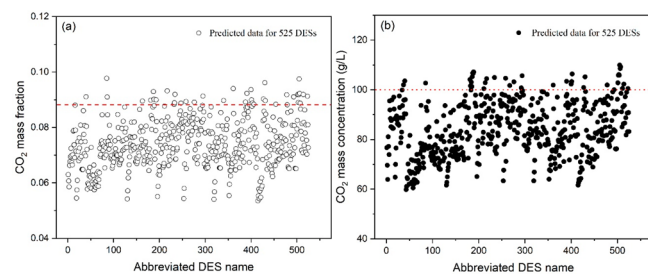


Figure 5. Predicted CO<sub>2</sub> solubilities in 525 hypothetical DESs at 298.15 K under 2.0 MPa, where the solubility is predicted in the form of (a) CO<sub>2</sub> mass fraction and (b) CO<sub>2</sub> mass concentration, respectively. Two red lines ( $y = 0.088$  and  $y = 100 \text{ g/L}$ ) indicate the maximum performance of DESs reported in the literature before.

in Table S7. The detailed data in Figure 5 can be found in Table S6.

Some combinations above the dashed red lines in Figure 5 are experimentally assessed, also summarized in Table S7. Within the investigated mixing ratios, 2,3,5,6-tetramethylpyrazine cannot form a clear liquid when it is mixed with menthol, methyl salicylate, vanillin, indole, or benzyl isothiocyanate. Eight stable and transparent liquids were selected (listed in Table 3) and subsequently experimentally characterized. Important properties were experimentally determined and are presented and discussed in the next section. For interested readers, some other combinations from Table S7, like indole–menthol (1:1), indole–lidocaine (1:1) and decanoic acid–2,3,5,6-tetramethylpyrazine (2:1) are also stable DESs and interesting for the extraction of organic and inorganic analytes from aqueous environments.<sup>65</sup>

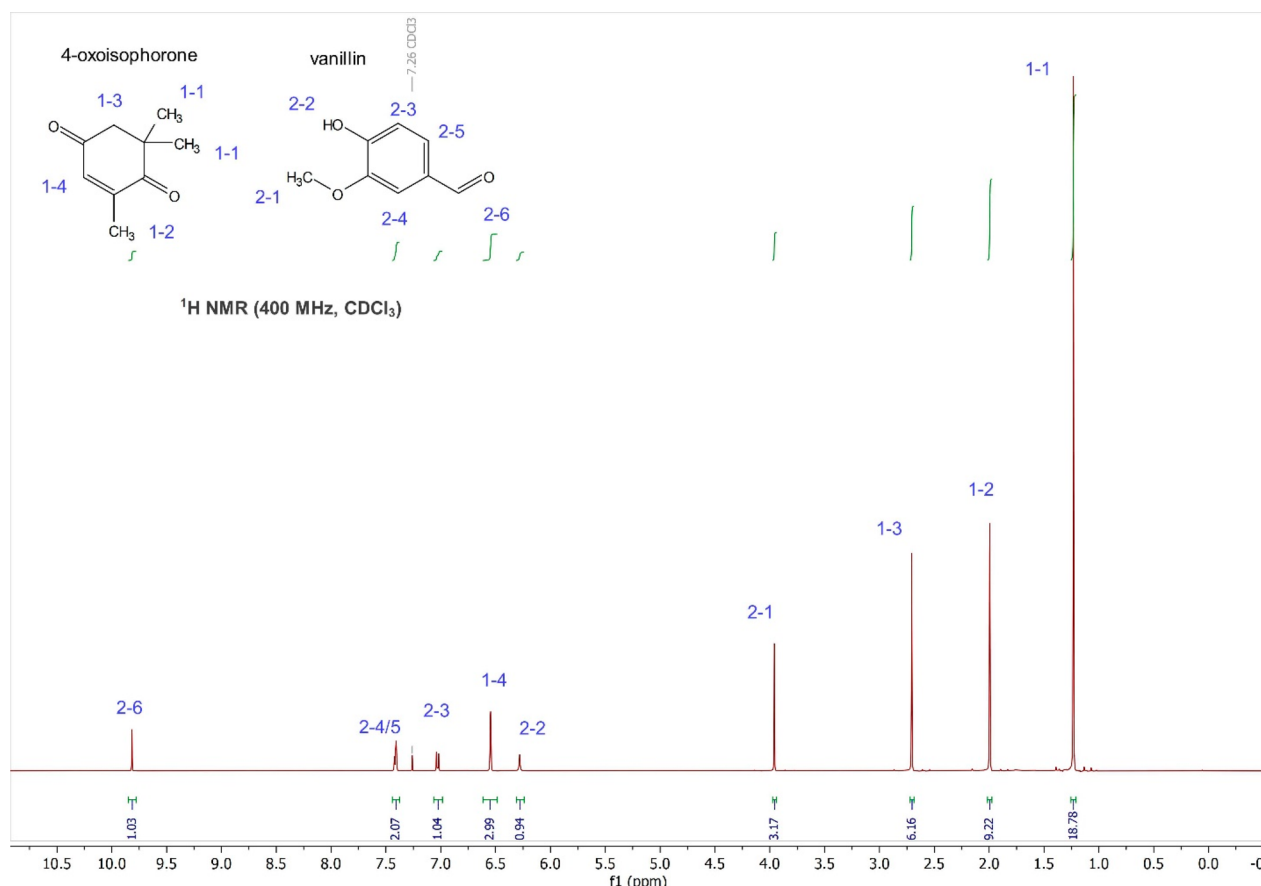
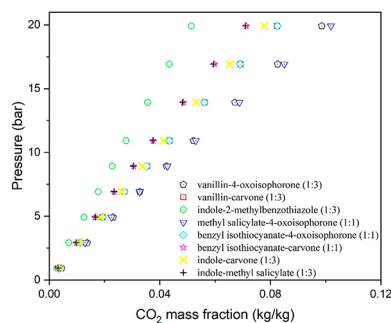
**Characterization of the Eight Selected Hydrophobic DESs for CO<sub>2</sub> Capture.** The constituents for the eight DESs presented in Table 3 can be derived from nature and are clean components according to the Chemwatch hazard ratings. Their hazards identifications and natural sources are summarized in Table S8. Except for possible skin contact problems of indole, other compounds are considered safe. To check whether reactions happen during the DES preparation, the <sup>1</sup>H NMR spectra of the HBD, HBA, and DES were compared. The experimental molar ratio of the HBD to HBA was also verified. Take vanillin-4-oxoisophorone (1:3) as an example. All of the signals were easily assigned to vanillin and 4-oxoisophorone by comparing with the <sup>1</sup>H NMR spectra of pure compounds (see Figure 6). Except for the peaks for HBD and HBA, no new peaks are found, demonstrating that no reactions occurred during the DES preparation. The peak of vanillin at 9.81 ppm, labeled with 2–6, has an integral value of 1.03, while the peak of 4-oxoisophorone at 6.54 ppm, labeled with 1–4 in Figure 6, has an integral value of 2.99, confirming that the molar ratio of the DES vanillin-4-oxoisophorone is indeed 1:3. Similar calculations were performed for all the other DESs, and the estimated ratios are all consistent with the expected theoretical molar ratios. The proton spectra for other seven DESs and the seven pure constituents are provided in Figures S3–S9 and S10–S16, respectively. No reactions were observed during the preparation of all these DESs.

To validate the predictions for the CO<sub>2</sub> solubility in these eight DESs, the CO<sub>2</sub> solubility was experimentally determined for these DESs at 298.15 K with an MSB, and the results are summarized in Figure 7. The highest CO<sub>2</sub> mass fraction of 10.19% under 2.0 MPa is found in the DES methyl salicylate–

**Table 3.** Measured Properties at 298.15 K for the Eight Promising Hydrophobic DESs

DES name	density (kg/m <sup>3</sup> )	viscosity (cP)	CO <sub>2</sub> mass fraction under 2.0 MPa (wt %)	CO <sub>2</sub> mass concentration under 2.0 MPa (g/L) <sup>a</sup>	water solubility (wt %) <sup>b</sup>
vanillin–4-oxoisophorone (1:3)	1078.79	17.12	9.86	106.37	4.54 ± 0.22
vanillin–carvone (1:3)	1018.38	6.933	8.24	83.91	3.02 ± 0.12
indole–2-methylbenzothiazole (1:3)	1158.98	7.442	5.14	59.57	3.28 ± 0.06
methyl salicylate–4-oxoisophorone (1:1)	1098.56	3.724	10.19	111.94	1.07 ± 0.04
benzyl isothiocyanate–4- oxoisophorone (1:1)	1071.25	3.456	8.25	88.38	0.69 ± 0.01
benzyl isothiocyanate–carvone (1:1)	1031.00	2.556	7.13	73.51	0.55 ± 0.02
indole–carvone (1:3)	984.77	4.028	7.78	76.62	1.52 ± 0.11
indole–methyl salicylate (1:3)	1162.4	4.194	7.10	82.53	0.60 ± 0.02

<sup>a</sup>No density change of the liquid during the CO<sub>2</sub> absorption is assumed. <sup>b</sup>Property at room temperature (22 ± 1 °C).

**Figure 6.** <sup>1</sup>H NMR of the DES vanillin-4-oxoisophorone (1:3).**Figure 7.** Experimental solubility of CO<sub>2</sub> in eight selected DESs at 298.15 K.

4-oxoisophorone (1:1), which is slightly above the originally predicted value of 8.99%. The slight underestimation of the CO<sub>2</sub> solubility by the COSMO-RS model could have been expected looking back at Figure 1d,e, showing that the CO<sub>2</sub> solubilities in ketones and esters are likely to be slightly underestimated, since ester and ketone groups are present in methyl salicylate and 4-oxoisophorone, respectively. The lowest measured CO<sub>2</sub> solubility is found in indole-2-methylbenzothiazole (1:3), which is only 5.14 wt % under 2.0 MPa. The highest relative deviation of 56.05% in the prediction is also found for this DES. The presence of benzene and heterocyclic rings in both DES constituents could account for this. On the one hand, the COSMO-RS method tends to overestimate CO<sub>2</sub> solubilities in aromatic compounds, as shown in Figure 1b. Moreover, the CO<sub>2</sub> solubilities in

heterocyclic compounds, such as pyridine and quinoline, are also likely to be overpredicted (see Figure 1h), where experimentally Henry's constants of 8.37 and 11.11 MPa were found at 298.15 K versus the predicted values of 7.57 and 7.18 MPa, respectively. The details of the experimental and predicted data at 298.15 K are summarized in Tables S9 and S10, respectively. The majority of the AARDs of the model prediction are less than 20%, reflecting overall good accuracy in the model predictions. It is also worth mentioning that the CO<sub>2</sub> solubilities in vanillin-4-oxoisophorone (1:3) and methyl salicylate-4-oxoisophorone (1:1) are comparable with the CO<sub>2</sub> solubility in Selexol. Considering the high CO<sub>2</sub> mass fractions in methyl salicylate-4-oxoisophorone (1:1), vanillin-4-oxoisophorone (1:3), vanillin-carvone (1:3), and benzyl isothiocyanate-4-oxoisophorone (1:1), the CO<sub>2</sub> solubilities in these four solvents were also experimentally determined at a higher temperature of 313.15 K, enabling the construction of thermodynamic models to describe the vapor liquid equilibrium of DES-CO<sub>2</sub> in a future work. As shown in Table S11, the CO<sub>2</sub> solubilities decrease with an increase in the temperature, as expected. The CO<sub>2</sub> mass fraction in methyl salicylate-4-oxoisophorone (1:1) under 2.0 MPa decreases from 10.19 to 7.79% when the temperature increases from 298.15 to 313.15 K, for example. The AARDs between the experimental data and COSMO-RS predictions at 313.15 K are close to the deviations at 298.15 K.

The density and viscosity of the eight DESs were measured between 293.15 and 353.15 K, as shown in Figures 8 and 9.

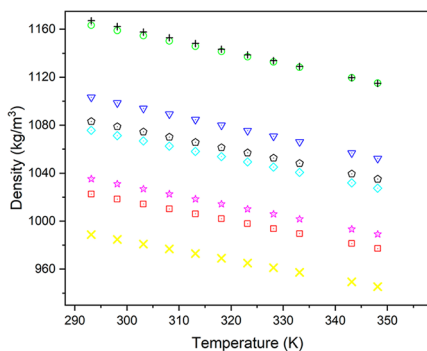


**Figure 8.** Experimentally determined densities for the selected eight DESs between 293.15 and 353.15 K. Symbols are (◇) vanillin-4-oxoisophorone (1:3); (□) vanillin-carvone (1:3); (○) indole-2-methylbenzothiazole (1:3); (▽) methyl salicylate-4-oxoisophorone (1:1); (◇) benzyl isothiocyanate-4-oxoisophorone (1:1); (☆), benzyl isothiocyanate-carvone (1:1); (×), indole-carvone (1:3); (+), indole-methyl salicylate (1:3).

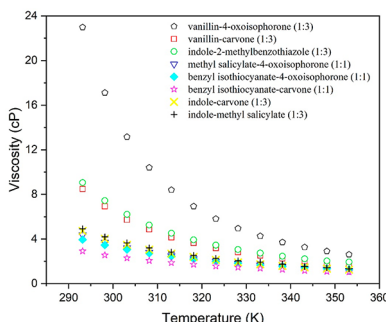


**Figure 9.** Experimentally determined viscosities for the selected eight DESs between 293.15 and 353.15 K.

Both decrease with increasing temperature. Except for the indole-carvone (1:3), the densities of all the other DESs at 298.15 K are above 1000 kg/m<sup>3</sup>. This is different compared to other DESs reported in the open literature,<sup>5</sup> whose densities are commonly smaller than 1000 kg/m<sup>3</sup>. The larger density of our new DESs brings about a longer residence time in the absorber when the solvent is applied for precombustion capture, slightly intensifying the process.<sup>6</sup> Even more exciting, due to the weak interaction strength between the constituents of these new DESs, except for vanillin-4-oxoisophorone (1:3), all viscosities of the newly developed DESs are less than 10 cP at 298.15 K, which is quite beneficial to achieve fast mass transfer during gas absorption. Take vanillin-4-oxoisophorone (1:3) as an example. It has the largest measured viscosity of (only) 17.12 cP at 298.15 K, while the predicted activity coefficients for its constituents at 298.15 K are 0.753 and 0.972, respectively. According to the modified Raoult's law, the weaker interactions between the constituents can enlarge the solvent volatility. Considering that the boiling point for all DES constituents are above 220 °C (Table S12), the newly developed DESs have a much lower volatility compared to conventional solvents like methanol and toluene. For the DESs, it is much more important to have a relatively low viscosity than it is to have a very low solvent volatility.<sup>6</sup>

Hydrophobic solvents can prevent water accumulation, maintain good solvent absorption capacity, and increase the energy efficiency of the power plant when applied in an advanced capture process. The newly developed DESs are superior to the reference absorbent in view of liquid hydrophobicity, since the Selexol solvent is miscible with water. The hydrophobicity of each DES was verified, the water solubility in the DES phase at room temperature was measured, and the results are shown in Table 3. The water solubility is very low (typically less than about 1–2%). When vanillin is involved in the formation of the DESs, somewhat larger amounts of water can be dissolved in DESs, where the water solubility in vanillin-4-oxoisophorone (1:3) and vanillin-4-oxoisophorone (1:3) is still below 5 wt %. Most likely vanillin is less hydrophobic. The DES concentration in the water phase was determined with GC-MS. The results are summarized in Table S13. All DESs prepared with 4-oxoisophorone and vanillin have higher organic contents, which can reach 3.72 wt %. The other DESs have a total organic content smaller than 1.0 wt %. Overall, it can be concluded that only small amounts of organics transfer to the water phase, and only small amounts of water transfer to the DES phase, when the DES is contacted with water.

Temperature-programmed thermogravimetric analyses were used to determine the degradation temperature of the DESs and are shown in Figure 10. They represent the weight loss of a DES over an increase in temperature. All the DESs show a one-step decay of weight loss and exhibit good thermal stability up to at least 373 K. The DESs prepared with 4-oxoisophorone have a slightly faster mass decrease rate. For vanillin-4-oxoisophorone (1:3), shown in Figure 10a, a fast mass loss rate was observed between 400 and 450 K, while the rate becomes slower because of the relatively high boiling point of vanillin. Table S14 provides an overview of the degradation temperatures from the thermograms of the DESs, which are all above 420 K. The volatilities of the best four DESs in view of CO<sub>2</sub> solubility were also determined at 298.15 and 313.15 K using TGA. The results are summarized in Table 4. The DES volatility highly depends on the selected constituents. It was

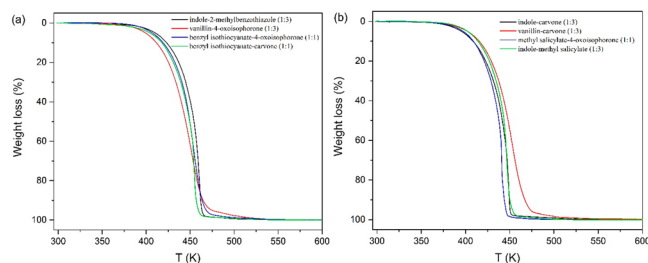


**Figure 10.** Panels (a) and (b) show thermograms of the eight DESs. The *x*-axis shows an increase in temperature (K), while the *y*-axis shows a loss in weight (%).

**Table 4. Total Vapor Pressure of Four Promising DESs and Comparison with Some Solvents**

solvent	total vapor pressure, Pa	
	at 298.15 K, Pa	at 313.15 K, Pa
vanillin-4-oxoisophorone (1:3)	3.07 ± 0.53	13.40 ± 0.90
vanillin-carvone (1:3)	7.43 ± 0.76	27.01 ± 1.64
methyl salicylate-4-oxoisophorone (1:1)	3.44 ± 0.14	16.51 ± 2.66
benzyl isothiocyanate-4-oxoisophorone (1:1)	3.37 ± 0.18	16.09 ± 0.39
Selexol <sup>57</sup>	0.097	
toluene <sup>a</sup>	3786.4	7886.25
decanoic acid–menthol (1:2) <sup>29</sup>		13.87
thymol–lidocaine (1:1) <sup>29</sup>		0.44

<sup>a</sup>From the NIST database.

reported in the literature that the strong hydrogen bond interactions between thymol and lidocaine result in a low volatility of thymol–lidocaine (1:1).<sup>29</sup> The volatilities of the newly developed DESs are comparable to the volatility of decanoic acid–menthol (1:2),<sup>29</sup> somewhat higher than the Selexol solvent and thymol–lidocaine (1:1), due to the relatively weak interaction strength between the DES constituents but still much lower compared to traditional solvents like toluene. The extent of solvent loses are quite minimal for these newly developed DESs, when used at relatively low temperatures. Alternatively, a washing section can be used to recover lost solvent on the top of the absorber.

**Prospects of Adopting COSMO-RS for the Prediction of the Density and Viscosity of DESs.** The pure compound density can be computed from a QSPR model in ADF, using descriptors from COSMO-RS calculations. The density of a DES was estimated from the densities of the HBD and HBA using eq 7.

$$\rho_{\text{DES}} = 1/(w_{\text{HBD}}/\rho_{\text{HBD}} + w_{\text{HBA}}/\rho_{\text{HBA}}) \quad (7)$$

where  $\rho$  and  $w$  represent the density and mass fraction, respectively. When applying this equation, volume expansion or contraction during mixing of the HBA and HBD is ignored. The accuracy of using COSMO-RS to estimate the densities for both pure compounds and DESs was verified by comparing the predicted densities with their experimental data. The descriptive statistics together with AARDs of the COSMO-RS predictions for a series of conventional solvents including alkanes, aromatic hydrocarbons, alcohol, acid and amide, and others have been summarized in Table S15, where a large range of solvent densities from 0.6 to 1.6 g/mL is considered. The results for nonionic DESs are compared in Table S16, while the parity plot of the model predictions vs the

experimental data for all the investigated solvents is shown in Figure 11. Almost all the points are within a relative error

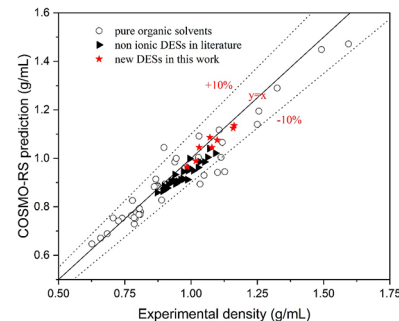


**Figure 11.** Parity plot of model predictions and experimental data for the density at 298.15 K for pure organic solvents, nonionic DESs in the literature, and the newly developed DESs in this work. The dotted lines represent a relative deviation of ±10%.

range of 10%, demonstrating that the COSMO-RS model predictions for pure compounds together with the ideal mixing rule (eq 7) can be used to accurately predict the densities of nonionic DESs.

We also tried to predict the DES viscosity with COSMO-RS. It has been reported by Lemaoui et al.<sup>19</sup> that the viscosity can also be estimated with QSPR models using the descriptors from COSMO-RS calculations. The  $\sigma$ -profiles are required to assign the descriptors. However, we have found that the  $\sigma$ -profiles are quite different when they are obtained with a different software. The comparison of  $\sigma$ -profiles obtained from ADF and COSMOtherm for lidocaine and oleic acid is presented in Figure S17. Both the  $\sigma$ -profiles consisted of 51 levels in the range of ±0.025 e Å<sup>-1</sup>. Huge differences can be observed between the two curves both in shape and in value. Thus, the correlations developed by Lemaoui et al. cannot be easily extended and used in another software, which may be related to a different parametrization of the COSMO-RS model in different software. Thus, it is important for researchers to get consistent  $\sigma$ -profiles when they are included in mathematical models.

## CONCLUSIONS

COSMO-RS was used for solvent screening and the design of new natural DESs for precombustion CO<sub>2</sub> capture. First, the accuracy of COSMO-RS calculations was validated by predicting the CO<sub>2</sub> solubility in various pure compounds and binary solvents. Next, the CO<sub>2</sub> solubility in 70 nonionic hydrophobic DESs from constituents reported in the open literature was screened, but none of these DESs can compete with the conventional Selexol solvent. Subsequently, 525 hypothetical DESs were obtained from binary combinations of 38 selected natural compounds. The DES constituents were selected for their high hydrophobicity and CO<sub>2</sub> affinity. The activity coefficients for the constituents were estimated with COSMO-RS, followed by the prediction of the CO<sub>2</sub> solubilities in theoretically feasible DESs. 58 promising hypothetical DESs were screened out, and eight DESs were selected and successfully prepared. The <sup>1</sup>H NMR spectra of the DESs show that no reactions prevail during their preparation. The DESs were further characterized in terms of CO<sub>2</sub> solubility, water solubility, density, viscosity, volatility, and thermal stability. Interestingly, 7 of the selected DESs have a density

at 298.15 K larger than 1.0 g/mL and exhibit a low intersolubility with water, have a relatively low volatility (comparable to decanoic acid-menthol (1:2)), and are thermally stable below 420 K. Vanillin-4-oxoisophorone (1:3) and methyl salicylate-4-oxoisophorone (1:1) are identified as very promising solvents for precombustion CO<sub>2</sub> capture, showing a comparable CO<sub>2</sub> solubility and viscosity to the conventional Selexol solvent but are much more environmentally benign. Finally, it has been demonstrated that COSMO-RS can be adequately used for solvent screening and design, where COSMO-RS can be used not only for the prediction of CO<sub>2</sub> and water solubilities but also for the prediction of the density of nonionic DESs using the simple ideal mixing rule. When using models from literature to predict liquid viscosity, consistent parametrization of the COSMO-RS model is required.

## ■ ASSOCIATED CONTENT

### SI Supporting Information

The Supporting Information is available free of charge at <https://pubs.acs.org/doi/10.1021/acssuschemeng.2c05090>.

Repeatability of the CO<sub>2</sub> solubility measurements (Figure S1); accuracy of CO<sub>2</sub> solubility prediction (Figure S2) in various solvents (Table S1); predicted CO<sub>2</sub> solubility in the nonionic DESs from the literature (Tables S2–S4); predicted activity coefficients and CO<sub>2</sub> solubility for the conceptual DESs (Tables S5 and S6); hazard ratings (Table S8), CO<sub>2</sub> solubility (Tables S9–S11), thermal stability (Tables S12 and S14); and water solubility (Table S13) as well as <sup>1</sup>H NMR (Figures S2–S16) for the final designed DESs (from Table S7) and their constituents; application of COSMO-RS for density prediction for the nonionic DESs (Tables S15, S16); comparison of σ-profiles from two different software (Figure S17) ([PDF](#))

## ■ AUTHOR INFORMATION

### Corresponding Author

Martin van Sint Annaland – *Chemical Process Intensification, Department of Chemical Engineering and Chemistry, Eindhoven University of Technology, 5600 MB Eindhoven, The Netherlands;*  [orcid.org/0000-0002-2903-7443](https://orcid.org/0000-0002-2903-7443); Email: [m.v.sintannaland@tue.nl](mailto:m.v.sintannaland@tue.nl)

### Authors

Kun Xin – *Chemical Process Intensification, Department of Chemical Engineering and Chemistry, Eindhoven University of Technology, 5600 MB Eindhoven, The Netherlands;*  [orcid.org/0000-0002-1965-0084](https://orcid.org/0000-0002-1965-0084)

Fausto Gallucci – *Inorganic Membranes and Membrane Reactors, Department of Chemical Engineering and Chemistry, Eindhoven University of Technology, 5600 MB Eindhoven, The Netherlands*

Complete contact information is available at:  
<https://pubs.acs.org/doi/10.1021/acssuschemeng.2c05090>

### Notes

The authors declare no competing financial interest.

## ■ ACKNOWLEDGMENTS

K.X. is grateful to the China Scholarship Council (CSC) for a Ph.D. Scholarship. We would also like to thank Ting Wan for

the help with the NMR study, and Machiel van Essen and Menno Houben for their help with the experiments.

## ■ REFERENCES

- Field, R. P.; Brasington, R. Baseline Flowsheet Model for IGCC with Carbon Capture. *Ind. Eng. Chem. Res.* **2011**, *50*, 11306–11312.
- Jansen, D.; Gazzani, M.; Manzolini, G.; Van Dijk, E.; Carbo, M. Pre-Combustion CO<sub>2</sub> Capture. *Int. J. Greenh. Gas Control* **2015**, *40*, 167–187.
- Fout, T.; Zoelle, A.; Kearns, D.; Turner, M.; Woods, M.; Kuehn, N.; Shah, V.; Chou, V.; Pinkerton, L. *Cost and Performance Baseline for Fossil Energy Plants Volume 1a: Bituminous Coal (PC) and Natural Gas to Electricity*, Revision 3; DOE/NETL-2010/1397; National Energy Technology Laboratory, 2015.
- Abbott, A. P.; Boothby, D.; Capper, G.; Davies, D. L.; Rasheed, R. K. Deep Eutectic Solvents Formed between Choline Chloride and Carboxylic Acids: Versatile Alternatives to Ionic Liquids. *J. Am. Chem. Soc.* **2004**, *126*, 9142–9147.
- Van Osch, D. J. G. P.; Dietz, C. H. J. T.; Van Spronsen, J.; Kroon, M. C.; Gallucci, F.; Van Sint Annaland, M.; Tuinier, R. A Search for Natural Hydrophobic Deep Eutectic Solvents Based on Natural Components. *ACS Sustain. Chem. Eng.* **2019**, *7* (3), 2933–2942.
- Xin, K.; Hashish, M.; Roghair, I.; van Sint Annaland, M. Process Simulation and Economic Analysis of Pre-Combustion CO<sub>2</sub> Capture With Deep Eutectic Solvents. *Front. Energy Res.* **2020**, *8*, 573267.
- Ghasem, N. CO<sub>2</sub> Removal from Natural Gas. In *Advances in Carbon Capture*; Elsevier, 2020; pp 479–501 DOI: [10.1016/b978-0-12-819657-1.00021-9](https://doi.org/10.1016/b978-0-12-819657-1.00021-9).
- Koronaios, P.; Stevenson, C.; Warman, S.; Enick, R.; Luebke, D. Thermally Stable Silicone Solvents for the Selective Absorption of CO<sub>2</sub> from Warm Gas Streams That Also Contain H<sub>2</sub> and H<sub>2</sub>O. *Energy Fuels* **2016**, *30* (7), 5901–5910.
- Current and Future Technologies for Gasification-Based Power Generation Volume 2: A Pathway Study Focused on Carbon Capture Advanced Power Systems R&D Using Bituminous Coal; National Energy Technology Laboratory, 2010.
- García, G.; Aparicio, S.; Ullah, R.; Atilhan, M. Deep Eutectic Solvents: Physicochemical Properties and Gas Separation Applications. *Energy Fuels* **2015**, *29* (4), 2616–2644.
- Siani, G.; Tiecco, M.; Di Profio, P.; Guernelli, S.; Fontana, A.; Ciulla, M.; Canale, V. Physical Absorption of CO<sub>2</sub> in Betaine/Carboxylic Acid-Based Natural Deep Eutectic Solvents. *J. Mol. Liq.* **2020**, *315*, 113708.
- Altamash, T.; Nasser, M. S.; Elhamarnah, Y.; Magzoub, M.; Ullah, R.; Qiblawey, H.; Aparicio, S.; Atilhan, M. Gas Solubility and Rheological Behavior Study of Betaine and Alanine Based Natural Deep Eutectic Solvents (NADES). *J. Mol. Liq.* **2018**, *256*, 286–295.
- Cui, G.; Lv, M.; Yang, D. Efficient CO<sub>2</sub> Absorption by Azolide-Based Deep Eutectic Solvents. *Chem. Commun.* **2019**, *55* (10), 1426–1429.
- Wang, Z.; Wang, Z.; Huang, X.; Yang, D.; Wu, C.; Chen, J. Deep Eutectic Solvents Composed of Bio-Phenol-Derived Superbase Ionic Liquids and Ethylene Glycol for CO<sub>2</sub> Capture. *Chem. Commun.* **2022**, *58* (13), 2160–2163.
- Gu, Y.; Hou, Y.; Ren, S.; Sun, Y.; Wu, W. Hydrophobic Functional Deep Eutectic Solvents Used for Efficient and Reversible Capture of CO<sub>2</sub>. *ACS Omega* **2020**, *5* (12), 6809–6816.
- Klamt, A.; Eckert, F. COSMO-RS: A Novel and Efficient Method for the a Priori Prediction of Thermophysical Data of Liquids. *Fluid Phase Equilib.* **2000**, *172* (1), 43–72.
- Haghbakhsh, R.; Bardool, R.; Bakhtyari, A.; Duarte, A. R. C.; Raeissi, S. Simple and Global Correlation for the Densities of Deep Eutectic Solvents. *J. Mol. Liq.* **2019**, *296*, 111830.
- Valderrama, J. O.; Robles, P. A. Critical Properties, Normal Boiling Temperatures, and Acentric Factors of Fifty Ionic Liquids. *Ind. Eng. Chem. Res.* **2007**, *46* (4), 1338–1344.
- Lemaoui, T.; Darwish, A. S.; Attoui, A.; Abu Hatab, F.; Hammoudi, N. E. H.; Benguerba, Y.; Vega, L. F.; Alnashef, I. M.

- Predicting the Density and Viscosity of Hydrophobic Eutectic Solvents: Towards the Development of Sustainable Solvents. *Green Chem.* **2020**, *22*, 8511–8530.
- (20) Liu, Y.; Yu, H.; Sun, Y.; Zeng, S.; Zhang, X.; Nie, Y.; Zhang, S.; Ji, X. Screening Deep Eutectic Solvents for CO<sub>2</sub> Capture With COSMO-RS. *Front. Chem.* **2020**, *8*, 82.
- (21) Alioui, O.; Benguerba, Y.; Alnashef, I. M. Investigation of the CO<sub>2</sub>-Solubility in Deep Eutectic Solvents Using COSMO-RS and Molecular Dynamics Methods. *J. Mol. Liq.* **2020**, *307*, 113005.
- (22) Liu, Y.; Dai, Z.; Zhang, Z.; Zeng, S.; Li, F.; Zhang, X.; Nie, Y.; Zhang, L.; Zhang, S.; Ji, X. Ionic Liquids/Deep Eutectic Solvents for CO<sub>2</sub> Capture: Reviewing and Evaluating. *Green Energy Environ.* **2021**, *6* (3), 314–328.
- (23) Klamt, A. Conductor-like Screening Model for Real Solvents: A New Approach to the Quantitative Calculation of Solvation Phenomena. *J. Phys. Chem.* **1995**, *99* (7), 2224–2235.
- (24) SCM. *Calculation of Properties — COSMO-RS 2019.3 Documentation*. [https://www.scm.com/doc/COSMO-RS/Calculation\\_of\\_properties.html](https://www.scm.com/doc/COSMO-RS/Calculation_of_properties.html) (accessed Aug 17, 2020).
- (25) Maiti, A. Theoretical Screening of Ionic Liquid Solvents for Carbon Capture. *ChemSusChem* **2009**, *2* (7), 628–631.
- (26) Palomar, J.; Ferro, V. R.; Torrecilla, J. S.; Rodríguez, F. Density and Molar Volume Predictions Using COSMO-RS for Ionic Liquids. An Approach to Solvent Design. *Ind. Eng. Chem. Res.* **2007**, *46* (18), 6041–6048.
- (27) SCM. *COSMO Result Files — Tutorials 2019.3 Documentation*. [https://www.scm.com/doc/Tutorials/COSMO-RS/COSMO\\_result\\_files.html#crs1](https://www.scm.com/doc/Tutorials/COSMO-RS/COSMO_result_files.html#crs1) (accessed Jul 31, 2020).
- (28) Zubeir, L. F.; Lacroix, M. H. M.; Kroon, M. C. Low Transition Temperature Mixtures as Innovative and Sustainable CO<sub>2</sub> Capture Solvents. *J. Phys. Chem. B* **2014**, *118* (49), 14429–14441.
- (29) Xin, K.; Roghair, I.; Gallucci, F.; van Sint Annaland, M. Total Vapor Pressure of Hydrophobic Deep Eutectic Solvents: Experiments and Modelling. *J. Mol. Liq.* **2021**, *325*, 115227.
- (30) PerkinElmer, Inc. *Characterization of Polymers Using TGA*. [https://resources.perkinelmer.com/lab-solutions/resources/docs/app\\_characterizationofpolymersusingtga.pdf](https://resources.perkinelmer.com/lab-solutions/resources/docs/app_characterizationofpolymersusingtga.pdf) (accessed Feb 21, 2021).
- (31) Kamgar, A.; Mohsenpour, S.; Esmaeilzadeh, F. Solubility Prediction of CO<sub>2</sub>, CH<sub>4</sub>, H<sub>2</sub>, CO and N<sub>2</sub> in Choline Chloride/Urea as a Eutectic Solvent Using NRTL and COSMO-RS Models. *J. Mol. Liq.* **2017**, *247*, 70–74.
- (32) Ab Manan, N.; Hardacre, C.; Jacquemin, J.; Rooney, D. W.; Youngs, T. G. A. Evaluation of Gas Solubility Prediction in Ionic Liquids Using COSMOthermX. *J. Chem. Eng. Data* **2009**, *54* (7), 2005–2022.
- (33) Fogg, P. G. *T. Carbon Dioxide in Non-Aqueous Solvents At Pressures Less Than 200 KPA*; Elsevier, 1992. DOI: [10.1016/c2009-0-00247-5](https://doi.org/10.1016/c2009-0-00247-5).
- (34) Gui, X.; Tang, Z.; Fei, W. Solubility of CO<sub>2</sub> in Alcohols, Glycols, Ethers, and Ketones at High Pressures from (288.15 to 318.15) K. *J. Chem. Eng. Data* **2011**, *56* (5), 2420–2429.
- (35) Li, Y.; Huang, W.; Zheng, D.; Mi, Y.; Dong, L. Solubilities of CO<sub>2</sub> Capture Absorbents 2-Ethoxyethyl Ether, 2-Butoxyethyl Acetate and 2-(2-Ethoxyethoxy)Ethyl Acetate. *Fluid Phase Equilib.* **2014**, *370*, 1–7.
- (36) Murrieta-Guevara, F.; Romero-Martinez, A.; Trejo, A. Solubilities of Carbon Dioxide and Hydrogen Sulfide in Propylene Carbonate, N-Methylpyrrolidone and Sulfolane. *Fluid Phase Equilib.* **1988**, *44* (1), 105–115.
- (37) Lenoir, J. Y.; Renault, P.; Renon, H. Gas Chromatographic Determination of Henry's Constants of 12 Gases in 19 Solvents. *J. Chem. Eng. Data* **1971**, *16* (3), 340–342.
- (38) Henni, A.; Tontiwachwuthikul, P.; Chakma, A. Solubilities of Carbon Dioxide in Polyethylene Glycol Ethers. *Can. J. Chem. Eng.* **2005**, *83* (2), 358–361.
- (39) Zhao, Z.; Xing, X.; Tang, Z.; Zhao, Y.; Fei, W.; Liang, X.; He, Z.; Zhang, S.; Guo, D. Solubility of CO<sub>2</sub> and H<sub>2</sub>S in Carbonates Solvent: Experiment and Quantum Chemistry Calculation. *Int. J. Greenh. Gas Control* **2017**, *59*, 123–135.
- (40) Li, Y.; Liu, Q.; Huang, W.; Yang, J. Below the Room Temperature Measurements of Solubilities in Ester Absorbents for CO<sub>2</sub> Capture. *J. Chem. Thermodyn.* **2018**, *127*, 71–79.
- (41) Gennaro, A.; Isse, A. A.; Vianello, E. Solubility and Electrochemical Determination of CO<sub>2</sub> in Some Dipolar Aprotic Solvents. *J. Electroanal. Chem.* **1990**, *289* (1–2), 203–215.
- (42) Li, Y.; Zheng, D.; Dong, L.; Xiong, B. Solubilities of Carbon Dioxide in 2-Methoxyethyl Acetate, 1-Methoxy-2-Propyl Acetate and 3-Methoxybutyl Acetate. *J. Chem. Thermodyn.* **2014**, *74*, 126–132.
- (43) Deng, D.; Han, G.; Jiang, Y.; Ai, N. Solubilities of Carbon Dioxide in Five Biobased Solvents. *J. Chem. Eng. Data* **2015**, *60* (1), 104–111.
- (44) Chal, C. P.; Paulaitis, M. E. Gas Solubilities of CO<sub>2</sub> in Heavy Hydrocarbons. *J. Chem. Eng. Data* **1981**, *26* (3), 277–279.
- (45) Li, X.; Jiang, Y.; Han, G.; Deng, D. Investigation of the Solubilities of Carbon Dioxide in Some Low Volatile Solvents and Their Thermodynamic Properties. *J. Chem. Eng. Data* **2016**, *61* (3), 1254–1261.
- (46) Xia, J.; Jödecke, M.; Kamps, A. P. S.; Maurer, G. Solubility of CO<sub>2</sub> in (CH<sub>3</sub>OH + H<sub>2</sub>O). *J. Chem. Eng. Data* **2004**, *49* (6), 1756–1759.
- (47) Dalmolin, I.; Skovroinski, E.; Biasi, A.; Corazza, M. L.; Dariva, C.; Oliveira, J. V. Solubility of Carbon Dioxide in Binary and Ternary Mixtures with Ethanol and Water. *Fluid Phase Equilib.* **2006**, *245* (2), 193–200.
- (48) Jödecke, M.; Kamps, Á. P. S.; Maurer, G. Experimental Investigation of the Solubility of CO<sub>2</sub> in (Acetone + Water). *J. Chem. Eng. Data* **2007**, *52* (3), 1003–1009.
- (49) Jödecke, M.; Pérez-Salado Kamps, Á.; Maurer, G. An Experimental Investigation of the Solubility of CO<sub>2</sub> in (N, N-Dimethylmethanamide + Water). *J. Chem. Eng. Data* **2012**, *57* (4), 1249–1266.
- (50) Merker, T.; Franke, N.; Gläser, R.; Schleid, T.; Hasse, H. Gas Solubility in Binary Liquid Mixtures: Carbon Dioxide in Cyclohexane + Cyclohexanone. *J. Chem. Eng. Data* **2011**, *56* (5), 2477–2481.
- (51) Jödecke, M.; Pérez-Salado Kamps, A.; Xia, J.; Maurer, G. An Experimental Investigation on the Solubility of CO<sub>2</sub> in Aqueous Solutions of Phenol. *Fluid Phase Equilib.* **2014**, *382*, 42–53.
- (52) Harifi-Mood, A. R. Solubility of Carbon Dioxide in Binary Mixtures of Dimethyl Sulfoxide and Ethylene Glycol: LFER Analysis. *J. Chem. Thermodyn.* **2020**, *141*, 105968.
- (53) Pazuki, G. R.; Pahlavanzadeh, H. Correlation and Prediction of the Solubility of CO<sub>2</sub> in a Mixture of Organic Solution Solvents. *Theor. Found. Chem. Eng.* **2005**, *39* (3), 240–245.
- (54) Höhler, F.; Deschermeier, R.; Rehfeldt, S.; Klein, H. Gas Solubilities of Carbon Dioxide in Methanol, Acetone, Mixtures of Methanol and Water, and Mixtures of Methanol and Acetone. *Fluid Phase Equilib.* **2018**, *459*, 186–195.
- (55) Gui, X.; Tang, Z.; Fei, W. Measurement and Prediction of the Solubility of CO<sub>2</sub> in Ester Mixture. *Low Carbon Econ.* **2011**, *2* (1), 26.
- (56) van Osch, D. J. G. P.; Dietz, C. H. J. T.; Warrag, S. E. E.; Kroon, M. C. The Curious Case of Hydrophobic Deep Eutectic Solvents: A Story on the Discovery, Design and Applications. *ACS Sustain. Chem. Eng.* **2020**, *8* (29), 10591–10612.
- (57) Tande, B.; Seames, W.; Benson, S. *Efficient Regeneration of Physical and Chemical Solvents for CO<sub>2</sub> Capture*; U.S. Department of Energy: Pittsburgh, PA, and Morgantown, WV (United States), 2013. DOI: [10.2172/1113825](https://doi.org/10.2172/1113825).
- (58) Zubeir, L. F.; Van Osch, D. J. G. P.; Rocha, M. A. A.; Banat, F.; Kroon, M. C. Carbon Dioxide Solubilities in Decanoic Acid-Based Hydrophobic Deep Eutectic Solvents. *J. Chem. Eng. Data* **2018**, *63*, 913.
- (59) Song, Z.; Hu, X.; Wu, H.; Mei, M.; Linke, S.; Zhou, T.; Qi, Z.; Sundmacher, K. Systematic Screening of Deep Eutectic Solvents as Sustainable Separation Media Exemplified by the CO<sub>2</sub> Capture Process. *ACS Sustain. Chem. Eng.* **2020**, *8* (23), 8741–8751.
- (60) Toprakçı, İ.; Pekel, A. G.; Kurtulbas, E.; Sahin, S. Special Designed Menthol-Based Deep Eutectic Liquid for the Removal of

Herbicide 2,4-Dichlorophenoxyacetic Acid through Reactive Liquid-Liquid Extraction. *Chem. Pap.* **2020**, *74*, 3995–4002.

(61) Khanh, P. N.; Trung, N. T. Understanding Interaction Capacity of CO<sub>2</sub> with Organic Compounds at Molecular Level: A Theoretical Approach. *Carbon Dioxide Chemistry, Capture and Oil Recovery* **2018**, *105*.

(62) Singh, P.; Pandey, A. K. Prospective of Essential Oils of the Genus *Mentha* as Biopesticides: A Review. *Frontiers in Plant Science*. **2018**, *9*, 1295.

(63) Schaeffer, N.; Abrantes, D. O.; Silva, L. P.; Martins, M. A. R.; Carvalho, P. J.; Russina, O.; Triolo, A.; Paccou, L.; Guinet, Y.; Hedoux, A.; Coutinho, J. A. P. Non-Ideality in Thymol + Menthol Type v Deep Eutectic Solvents. *ACS Sustain. Chem. Eng.* **2021**, *9* (5), 2203–2211.

(64) Hayyan, A.; Hadj-Kali, M. K.; Salleh, M. Z. M.; Hashim, M. A.; Rubaidi, S. R.; Hayyan, M.; Zulkifli, M. Y.; Rashid, S. N.; Mirghani, M. E. S.; Ali, E.; Basirun, W. J. Characterization of Tetraethylene Glycol-Based Deep Eutectic Solvents and Their Potential Application for Dissolving Unsaturated Fatty Acids. *J. Mol. Liq.* **2020**, *312*, 113284.

(65) Lee, J.; Jung, D.; Park, K. Hydrophobic Deep Eutectic Solvents for the Extraction of Organic and Inorganic Analytes from Aqueous Environments. *TrAC - Trends in Analytical Chemistry*. **2019**, *118*, 853–868.

## □ Recommended by ACS

### Effect of Hydrogen Bonds on CO<sub>2</sub> Capture by Functionalized Deep Eutectic Solvents Derived from 4-Fluorophenol

Zonghua Wang, Dezhong Yang, *et al.*

APRIL 07, 2023

ACS SUSTAINABLE CHEMISTRY & ENGINEERING

READ ▶

### CO<sub>2</sub> Separation Using Supported Deep Eutectic Liquid Membranes Based on 1,2-propanediol

Bartosz Nowosielski, Iwona Cichowska-Kopczyńska, *et al.*

MARCH 01, 2023

ACS SUSTAINABLE CHEMISTRY & ENGINEERING

READ ▶

### Mechanism Study of Imidazole-Type Deep Eutectic Solvents for Efficient Absorption of CO<sub>2</sub>

Shengyou Shi, Xiangwei Liu, *et al.*

DECEMBER 12, 2022

ACS OMEGA

READ ▶

### Imidazole-Monoethanolamine-Based Deep Eutectic Solvent for Carbon Dioxide Capture: A Combined Experimental and Molecular Dynamics Investigation

Fatma R. Al-Fazari, Suhaib Al Ma'awali, *et al.*

APRIL 05, 2023

JOURNAL OF CHEMICAL & ENGINEERING DATA

READ ▶

Get More Suggestions >